HHS Public Access

Author manuscript

Toxicol Appl Pharmacol. Author manuscript; available in PMC 2023 May 04.

Published in final edited form as:

Toxicol Appl Pharmacol. 2021 April 15; 417: 115470. doi:10.1016/j.taap.2021.115470.

Myeloid cell dynamics in bleomycin-induced pulmonary injury in mice; effects of anti-TNFα antibody

Alessandro Venosa[a,1], **James G. Gow**[b,1], **Sheryse Taylor**[c], **Thea N. Golden**[d], **Alexa Murray**[c], **Elena Abramova**[c], **Rama Malaviya**[c], **Debra L. Laskin**[c], **Andrew J. Gow**[c,*]

[a]Department of Pharmacology and Toxicology, University of Utah, Salt Lake City, UT 84112, USA

[b]Dartmouth College, Hanover, NH 03755, USA

[c]Department of Pharmacology and Toxicology, Ernest Mario School of Pharmacy, Rutgers University, Piscataway, NJ 08854, USA

[d]Center for Research on Reproduction and Women's Health, Perelman School of Medicine, University of Pennsylvania, Philadelphia, PA 18015, USA

Abstract

Bleomycin is a cancer therapeutic known to cause lung injury which progresses to fibrosis. Evidence suggests that macrophages contribute to this pathological response. Tumor necrosis factor (TNF)α is a macrophage-derived pro-inflammatory cytokine implicated in lung injury. Herein, we investigated the role of TNFα in macrophage responses to bleomycin. Treatment of mice with bleomycin (3 U/kg, i.t.) caused histopathological changes in the lung within 3 d which culminated in fibrosis at 21 d. This was accompanied by an early (3–7 d) influx of $CD11b^+$ and $iNOS^+$ macrophages into the lung, and $Arg\text{-}1^+$ macrophages at 21 d. At this time, epithelial cell dysfunction, defined by increases in total phospholipids and SP-B was evident. Treatment of mice with anti-TNFα antibody (7.5 mg/kg, i.v.) beginning 15–30 min after bleomycin, and every 5 d thereafter reduced the number and size of fibrotic foci and restored epithelial cell function. Flow cytometric analysis of $F4/80^+$ alveolar macrophages (AM) isolated by bronchoalveolar lavage and interstitial macrophages (IM) by tissue digestion identified resident ($CD11b^-$ $CD11c^+$) and immature infiltrating ($CD11b^+CD11c^-$) AM, and mature ($CD11b^+CD11c^+$) and immature ($CD11b^+CD11c^-$) IM subsets in bleomycin treated mice. Greater numbers of mature ($CD11c^+$)

*Corresponding author at: Department of Pharmacology and Toxicology, Ernest Mario School of Pharmacy, Rutgers University, 160 Frelinghuysen Road, Piscataway, NJ 08854-8020, USA. gow@pharmacy.rutgers.edu (A.J. Gow).

[1]The authors contributed equally to this manuscript.

Credit author statement

Alessandro Venosa Conceptualization; Data curation, Formal analysis; Visualization; Writing - original draft; Writing - review & editing.

James Gow Data curation, Formal analysis; Validation; Methodology; Writing - original draft.

Sheryse Taylor Data curation, Formal analysis; Methodology.

Thea Golden Data curation, Formal analysis; Methodology; Visualization; Writing - original draft; Writing - review & editing.

Alexa Murray Data curation, Formal analysis; Methodology.

Elena Abramova Formal analysis; Methodology.

Rama Malaviya Conceptualization; Data curation.

Debra Laskin Supervision; Writing - review & editing.

Andrew Gow Conceptualization; Project administration; Funding acquisition; Writing - original draft; Writing - review & editing.

Declaration of Competing Interest

The authors declare that they have no known competing financial interests or personal relationships that could have appeared to influence the work reported in this paper.

infiltrating ($CD11b^+$) AM expressing the anti-inflammatory marker, mannose receptor (CD206) were observed at 21 d when compared to 7 d post bleomycin. Mature proinflammatory ($Ly6C^+$) IM were greater at 7 d relative to 21 d. These cells transitioned into mature anti-inflammatory/pro-fibrotic ($CD206^+$) IM between 7 and 21 d. Anti-TNFα antibody heightened the number of $CD11b^+$ AM in the lung without altering their activation state. Conversely, it reduced the abundance of mature proinflammatory ($Ly6C^+$) IM in the tissue at 7 d and immature pro-fibrotic IM at 21 d. Taken together, these data suggest that TNFα inhibition has beneficial effects in bleomycin induced injury, restoring epithelial function and reducing numbers of profibrotic IM and the extent of pulmonary fibrosis.

1. Introduction

Bleomycin is a highly effective chemotherapeutic against carcinomas and sarcomas (Yu et al., 2016); however, the fact that it causes pulmonary fibrosis has limited its use. This adverse effect has been leveraged to the point that bleomycin is now widely used as an experimental model of acute lung injury and pulmonary fibrosis (Williamson et al., 2015). An advantage of the model is that a single exposure to bleomycin drives the sequential and distinct phases of acute inflammation, resolution, and repair. A number of studies have examined how interfering with these injury phases can alter the outcome of pulmonary fibrosis (Koyama et al., 2019; Saito et al., 2019; Shariati et al., 2019; Zhang et al., 2019).

While the acute inflammatory phase of bleomycin-induced pulmonary toxicity is dominated by neutrophil activity, the later phases of injury progression, resolution and fibrogenesis are regulated by macrophages (Misharin et al., 2017). These cells include tissue resident macrophages, which are pivotal in homeostatic maintenance, and monocyte-derived inflammatory macrophages localized in the alveolar and interstitial spaces, which respond to tissue injury (Misharin et al., 2013; Gibbings et al., 2017). Inflammatory macrophages have been broadly classified into two distinct populations, M1/proinflammatory and M2/anti-inflammatory macrophages. Whereas M1 macrophages produce proinflammatory mediators including tumor necrosis factor (TNF)-α, interleukin (IL)-1, IL-6, and IL-12 and express inducible nitric oxide synthase (iNOS), M2 macrophages release mediators such as IL-4, IL-10, IL-13, and TGFβ that downregulate inflammation and initiate wound repair. Excessive release of mediators by M1 and/or M2 macrophages can exacerbate tissue injury and induce fibrosis (Wynn and Vannella, 2016). Previous studies have shown that during the acute inflammatory phase of bleomycin-induced lung injury, M1 macrophages dominate, while during the resolution/fibrogenic phase, M2 macrophages are the major subset (Walters and Kleeberger, 2008).

TNFα is a proinflammatory cytokine produced mainly by macrophages in response to tissue injury; it has been implicated in the pathogenesis of a variety of pulmonary diseases including fibrosis (Malaviya et al., 2017). In addition to promoting myeloid cell recruitment and differentiation, TNFα induces oxidative and nitrosative stress, as well as necrosis, apoptosis, angiogenesis, and tissue remodeling (Aggarwal, 2003; Mukhopadhyay et al., 2006; Blaser et al., 2016). Studies have demonstrated that blocking TNFα activity using pharmacologic or genetic modulation blunts tissue injury and inflammation induced by

diverse pulmonary toxicants (Piguet and Vesin, 1994; Bhalla et al., 2002; Malaviya et al., 2015; Malaviya et al., 2017; Ge et al., 2018; Laskin et al., 2019).

In the current studies, we combined histologic analysis with techniques in immunohistochemistry and flow cytometry to assess the effects of TNFα blockade on macrophage accumulation and activation in the lung following bleomycin-induced injury, resolution and fibrogenesis. We found that bleomycin administration was associated with sequential accumulation of pro- and anti-inflammatory alveolar and interstitial macrophages in the lung. Anti-TNFα antibody administration was found to alter interstitial macrophage activation and improve alveolar epithelial type II cell function. These findings provide new insights into the potential therapeutic benefit of blocking TNFα during pulmonary injury and fibrogenesis.

2. Methods

2.1. Animals and treatments

C57BL/6 J male mice (8 week old, The Jackson Laboratories, Bar Harbor, ME) were housed in filter top microisolation cages and provided food and water ad libitum; they received humane care in compliance with the guidelines outlined in the Guide for the Care and Use of Laboratory Animals, published by the National Institutes of Health. Mice were treated with 50 μL bleomycin (3 U/kg) or control (saline solution, 0.9% NaCl) by intratracheal instillation. In separate studies, bleomycin exposure was followed 15–30 min later by tail vein administration of chimeric monoclonal IgG2ακ anti-mouse anti-TNFα antibody (7.5 mg/kg, *i.v.*, Janssen Pharmaceuticals Inc., Spring House, PA) or PBS control. Antibody was subsequently administered once every 5 days.

2.2. Bronchoalveolar lavage fluid (BAL) and cell collection

Animals were euthanized by *i.p.* injection of Sleepaway (2 mL/kg, Fort Dodge Animal Health, Fort Dodge, IA) 3 d, 7 d or 21 d post saline control or bleomycin. Anti-TNFα antibody treated study groups were euthanized at 7 d and 21 d post bleomycin. BAL was collected by slowly instilling and withdrawing (x 5) 1 mL of ice-cold saline into the lung through a cannula inserted into the trachea. BAL was centrifuged (300 *g*, 8 min), and supernatants analyzed for protein and phospholipid. Cell- free supernatants were assayed for protein content using a BCA protein assay kit (Pierce Biotechnologies Inc., Rockford, IL) with bovine serum albumin as the standard. Cell pellets were resuspended in 500 μL of PBS, enumerated using a Beckman Coulter counter (Indianapolis, IN), and processed for flow cytometric analysis.

2.2.1. Interstitial macrophage isolation—The right lung lobes were finely diced and incubated with collagenase IV (2 mg/mL) at 37 °C in RPMI media containing 5% fetal bovine serum (FBS) for 30 min, with gentle shaking every 5 min. The lung digests were filtered through a 70 μm cell strainer, washed, centrifuged, and cell pellets resuspended in 100 μL of Ca^{++}/Mg^{++} free PBS containing 2% FBS and 1 mM EDTA. Cells were then treated with 0.25 μg rat anti-mouse CD16/32 (clone 93; BioLegend, San Diego, CA) for 5 min at room temperature to block nonspecific binding. An EasySep PE Positive Selection

Kit (Stem Cell Technologies) was used to isolate F4/80$^+$ macrophages from lung digests following the manufacturer's directions. Briefly, the filtered lung digest was incubated with PE conjugated anti-F4/80 antibody (1.5 μg/mL) for 15 min at room temperature. A Selection Cocktail (100 μL/mL) was added to the cell suspension followed by Magnetic Particles (50 μL/mL) and incubation for 10 min at room temperature. The samples were then diluted with PBS containing 2% FBS and 1 mM EDTA and F4/80$^+$ cells isolated by magnetic separation.

2.2.2. Flow cytometric analysis—BAL cells and tissue digest single cell suspensions were resuspended in 100 μL of staining buffer. This was followed by 30 min incubation with FITC-conjugated anti-mouse CD206 (1:100, clone C068C2; BioLegend), PerCP/Cy5.5 conjugated anti-mouse Ly-6C (1:100, clone HK1.4 BioLegend), APC conjugated anti-mouse CD11b (1:100, clone M1/70; BioLegend), and/or Alexa Fluor 700 conjugated anti-mouse CD11c (1:100, clone N418; BioLegend) antibodies or appropriate isotype controls at 4 °C and then with eFluor 780-conjugated fixable viability dye (1:1000, eBiosciences). In experiments with cells collected by lavage, cells were also incubated with PE-conjugated anti-mouse F4/80 antibody (1:100, clone BM8; eBiosciences, San Diego, CA). Cells were washed and fixed in 2% paraformaldehyde and analyzed on a Gallios flow cytometer (Beckman Coulter, Brea, CA). Cell populations were identified based on forward and side scatter followed by doublet discrimination of live cells. Data were analyzed using Beckman Coulter Kaluza (version 1.2) software. Viable F4/80$^+$ BAL cells were initially analyzed for expression of CD11c followed sequentially by CD11b and CD206 (mannose receptor); viable tissue digest cells were analyzed for expression of CD11b followed sequentially by CD11c and CD206. The number of cells within each subpopulation was calculated from the percentage of positive cells relative to the total number of F4/80$^+$ viable cells recovered.

2.3. Histology and immunohistochemistry

For preparation of histologic sections, the left lobe was instilled with 3% paraformaldehyde, removed, fixed in 3% paraformaldehyde overnight at 4 °C, and then transferred to 50% ethanol. Sections (5 μm) were prepared, stained with Hematoxylin and Eosin (H&E), and analyzed microscopically. Semi-quantitative histological scoring (0 = healthy; 1 = small foci of injury affecting up to 20% of lung tissue; 2 = increasing numbers of injury foci, perivascular infiltrate and edema affecting approximately 20–40% of lung tissue; 3 = increasing numbers of injury foci, perivascular infiltrate and edema affecting approximately 40–60% of lung tissue; 4 = increasing numbers of injury foci, perivascular infiltrate and edema affecting approximately 60–80% of lung tissue; 5 ≥80% affected lung with extensive edema and perivascular edema) was based on blinded evaluation of number and size of foci of injury, perivascular infiltrate, and edema. Lungs were also assessed for fibrosis using a scaling system previously reported by Izbicki, et al. (Izbicki et al., 2002). Finally, morphological measurements of percentage airspace, alveolar wall width, and number of nuclei per high powered field were made in order to assess lung architectural changes in response to bleomycin. For immunohistochemistry, tissue sections were deparaffinized with xylene and hydrolyzed by passing through a gradient of ethanol (100–50%) followed by water. After antigen retrieval with citrate buffer (10.2 mM sodium citrate, 0.05% Tween 20, pH 6.0, 10 min) and quenching of endogenous peroxidase with 3% hydrogen peroxide in methanol (30 min), sections were incubated for 2 h at room temperature with 5% serum

to block nonspecific binding. This was followed by overnight incubation at 4 °C in a humidified chamber with a rabbit polyclonal anti-YM-1 (1:800, Stem Cell Technologies, Vancouver, Canada), CD11b, (1:1000, Abcam, Cambridge, MA), inducible nitric oxide synthase (iNOS, 1:150, Abcam), arginase-1 (Arg-1, 1:1500, Abcam) or the appropriate serum/IgG controls diluted in blocking buffer. Sections were then washed and incubated at room temperature for 30 min with biotinylated secondary antibody (Vectastain Elite ABC kit, Vector Laboratories, Burlingame, CA). Binding was visualized using a Peroxidase Substrate Kit DAB (Vector Laboratories). Random sections from at least three mice per treatment group were assessed for each antibody.

2.4. Surfactant protein analyses

BAL was separated into hydrophobic large aggregate (LA) and hydrophilic small aggregate (SA) fractions by ultracentrifugation (20,000 *g*) for 1 h. Phospholipid content in the LA fraction was quantified by measuring inorganic phosphate content acquired from the lipid phase (Bligh and Dyer, 1959; Rouser et al., 1966). Total protein content in LA and SA fractions was measured by the Bradford method using bovine albumin as a standard. Relative surfactant protein content was determined by western blotting. SP-D content was measured in whole BAL, while SP-B content was measured in the LA fraction reconstituted in sodium chloride saline solution (NaCl, 0.9%). Samples of denatured BAL or LA fraction (2 μg protein) were reduced with dithiothreitol and then fractionated onto 4–12% Bis-Tris (SP-D) or 3–8% tris-acetate (SP-B) polyacrylamide gradient gels (Invitrogen, Carlsbad, CA). Proteins were transferred to PVDF membranes, blocked in 10% milk for 40 min and then incubated with anti-SP-D (Cao et al., 2004) or anti- SP-B (Guttentag et al., 1997) antibodies (1:20,000) provided by Dr. Michael Beers (University of Pennsylvania, Philadelphia, PA). The membranes were subsequently incubated with HRP-conjugated secondary antibody (1:5000) (Santa Cruz Biotechnology, Santa Cruz CA) and developed following incubation with Amersham ECL Plus (GE Healthcare Bio- sciences, Pittsburgh, PA); intensity was quantified using Kodak 440 imaging platform. Background corrected SP-B and SP-D signal intensity was determined for each sample and reported as mean ± SD, normalized to mean intensity of control within each blot.

2.5. Statistical analysis

Each experimental group consisted of 5–6 animals. Data were analyzed using GraphPad Prism V6.01 (GraphPad Software Inc., La Jolla, CA). Histological scoring data were analyzed using Kruskal–Wallis non-parametric one-way ANOVA followed by Mann–Whitney Rank Sum post-hoc test. A one-way ANOVA with no matching between groups and Tukey's multiple comparisons, or unpaired *t*-test (unequal variance) was used to analyze differences between groups. Western blot data was analyzed by one-way ANOVA followed by Dunnett's post-hoc test. A p value of ≤ 0.05 was considered statistically significant.

3. Results

3.1. Bleomycin induces persistent inflammatory changes in the lung

Immunohistochemical analysis of $CD11b^+$ myeloid cell infiltration into the lung revealed a time related increase at 3 d post administration of bleomycin, with peak influx at

7 d, a time point previously described as representative of the transition from acute inflammation to tissue remodeling (Guo et al., 2016). At 21 d, a time associated with fibrogenesis, $CD11b^+$ cells were still present in the lung (Fig. 1, left panels). This increase in $CD11b^+$ cells was reflected in morphological analysis which revealed increased cellularity at both 7 and 21 days post bleomycin, but no significant alteration of alveolar structure (supplemental Fig. 1). Phenotypic analysis of inflammatory cells in the lung revealed time related increases in expression of the proinflammatory protein iNOS beginning 3 d after bleomycin administration and persisting up to 21 d (Fig. 1, center panels). In contrast, Arg-1 expression, a marker associated with anti-inflammatory/profibrotic activation, was only observed 21 d post bleomycin exposure (Fig. 1, right panels).

3.2. Effects of anti-TNFα antibody on bleomycin-induced lung histopathology and inflammatory cell accumulation in the lung

Consistent with previous studies (Casey et al., 2005), at 7 days post bleomycin administration, there was an accumulation of inflammatory cells within the peribronchial and perivascular regions of the lung (Fig. 2A). This was accompanied by collagen deposition, as evidenced by trichrome staining, a response which increased with time becoming pronounced by 21 d (Fig. 2B and C). Anti-TNFα antibody, administered immediately following bleomycin and every 5 days thereafter, had no significant effect on inflammatory cell accumulation in the lung at 7 d or 21 d or on the extent of alveolar epithelial disruption and perivascular edema at 7 d (Fig. 2). This was confirmed by unbiased analysis of alveolar wall thickness and alveolar air space volume, which was not significantly changed by Anti-TNFα treatment within bleomycin exposed cohorts (Supp. Fig. 2). Conversely, analysis of fibrotic foci indicated that anti-TNFα therapy effectively reduced the extent of tissue remodeling and fibrosis at 21 d (Fig. 2A and C).

3.3. Effects of anti-TNFα antibody on the phenotype of macrophages responding to bleomycin-induced lung injury

We next analyzed the effects of anti-TNFα antibody on the phenotype of activated macrophage subsets recovered from BAL and tissue digests at 7 d and 21 d post bleomycin exposure, representing peak inflammation and tissue remodeling/fibrosis, respectively. Significantly greater numbers of $F4/80^+CD11b^+$ infiltrating macrophages were observed in BAL at 21 d relative to 7 d post bleomycin administration (Fig. 3A and B); this was augmented by anti-TNFα antibody treatment. These infiltrating cells were further characterized for expression of the macrophage maturity marker, CD11c, and CD206, a scavenger receptor known to be linked to anti-inflammatory/profibrotic macrophages (Roszer, 2015; Soldano et al., 2016). A significant increase in $CD206^+$ infiltrating macrophages ($F4/80^+CD11b^+$) expressing the CD11c maturity marker was observed at 21 d, compared to the same cell population analyzed 7 d post bleomycin; anti-TNFα antibody had no major effect on these cells (Fig. 3C and D). An increase in $CD206^+$ alveolar macrophages ($F4/80^+CD11b^-$ $CD11c^+$) was also noted at 21 d, when compared to 7 d; this was correlated with a decrease in $CD206^-$ alveolar macrophages (Fig. 3E and F). Anti-TNFα antibody had no effect on these cell populations.

To gain better perspective of changes in macrophage composition at the interstitial level, we next analyzed lung digests. In these studies, F4/80$^+$ cells were magnetically selected and analyzed for CD11b, CD11c, CD206and Ly6C to differentiate mature (CD11b$^+$CD11c$^+$) and (CD11b$^+$CD11c$^-$) immature interstitial macrophages, from resident alveolar macrophages (CD11b$^-$ CD11c$^+$) (Fig. 4A). No significant differences were observed in the relative percentage of CD11b$^+$ cells or CD11b$^+$CD11c$^+$ interstitial macrophages between 7 d and 21 d post-bleomycin, or between anti-TNFα treated mice and bleomycin + saline treated mice (Fig. 4B, C and D). In contrast, the relative abundance of CD11b$^+$CD11c$^-$ immature interstitial macrophages was reduced at 21 d relative to 7 d after administration of anti-TNFα antibody (Fig. 4E). Following bleomycin administration, we also noted an increase in both immature CD11b$^+$CD11c$^-$ and mature CD11b$^+$CD11c$^+$ interstitial macrophages expression of the anti-inflammatory scavenger receptor CD206, at 21 d relative to 7d (Fig. 5A and C). Whereas anti-TNFα antibody had no effect on mature interstitial macrophage expression of CD206 at 21 d post bleomycin, it blunted increases in CD206 expression on immature interstitial macrophages (Fig. 5A and B). Further analysis of digested cells pre-gated on CD11b$^+$ expression showed that the relative abundance of mature proinflammatory CD11c$^+$Ly6C$^+$ interstitial macrophages was maximal 7 d post bleomycin; anti-TNFα antibody significantly reduced their abundance at 7 days with no effect at 21 d (Fig. 5D and F). Immunohistochemical analysis of the lung for the anti- inflammatory/profibrotic macrophage protein, YM-1 showed increased and persistent expression in both groups, with no differences in accumulation patterns or numbers (Fig. 5G).

3.4. Effects of anti-TNFα antibody on bleomycin-induced alterations in lung phospholipids and surfactant proteins

Previous studies have demonstrated that surfactant producing type II alveolar epithelial cells are highly sensitive to bleomycin (Barkauskas and Noble, 2014). Injury to type II cells is associated with reduced levels of lipid-rich alveolar surfactants lining the respiratory epithelium. In further studies we analyzed the effects of anti-TNFα antibody administration on bleomycin induced alterations in lung phospholipids, as well as levels of inflammatory associated SP-D and the “true surfactant”, SP-B. Low levels of phospholipids were detected in LA fractions of BAL from control mice (Fig. 6A). Whereas bleomycin had no effect on total BAL phospholipids levels 21 d after exposure, anti-TNFα antibody treatment caused a significant increase in phospholipid levels (Fig. 6A). Further analysis of BAL lipids revealed low levels of SP-D in control mice (Fig. 6B). As observed with total phospholipids, although bleomycin had no effect on SP-D or SP-B levels at 21 d post exposure, anti-TNFα antibody caused a two- and five-fold increase, respectively, in levels of these proteins in BAL (Fig. 6B and C). Consistent with the notion that bleomycin promotes type II cell dysfunction, the ratio of total phospholipids to SP-B ratio, considered a biomarker of surfactant lipid homeostasis, was increased 21 d following bleomycin administration (12 ±3.8 g/A.U. for control vs 27 ± 9.6 g/A.U. for bleomycin) (Fig. 6D). Anti-TNFα antibody treatment reduced the phospholipid/SP-B ratio to control levels (11 ± 4.8 μg/A.U.), suggesting normalization of type II cell function.

4. Discussion

Intratracheal bleomycin administration is a well-established model of acute lung injury that progresses to fibrosis (Hay et al., 1991; Moeller et al., 2008). The pathologic process of injury involves both inflammatory activation and repair processes (Hay et al., 1991). Herein, we showed that the progressive changes that occur within the lung following bleomycin administration are accompanied by changes in inflammatory macrophage accumulation and activation within the alveolar space and the interstitium. We also demonstrate that inhibition of TNFα signaling reduces the extent of bleomycin induced fibrosis, normalizes type II cell function, and modifies lung macrophage activation. These findings provide important insights on the inflammatory processes mediating fibrogenesis.

The recruitment of inflammatory cells to the lung following bleomycin administration occurs within 3 d as evidenced by the appearance of cells bearing the mobility marker, $CD11b^+$ in the tissue. These cells persisted for at least 21 d, a time associated with the resolution of inflammation and fibrogenesis, consistent with a role of infiltrating myeloid cells in both phases of the inflammatory response (Braga et al., 2016; Venosa et al., 2016). Our findings of macrophage iNOS expression 3–21 days post bleomycin, demonstrate persistent pro-inflammatory activation in the lung (Kobayashi, 2010). Conversely, the prototypical anti-inflammatory/profibrotic marker, Arg-1, was only expressed in inflammatory cells at 21 d, a time we showed is consistent with fibrosis, as evidenced by trichrome staining (Yang and Ming, 2014). Together, these observations support the notion that the activation state of macrophages responding to bleomycin injury is best represented by a spectrum rather than an dichotomous phenotype (i.e. only M1 or M2) (Mosser and Edwards, 2008). These findings prompted us to evaluate shifts in macrophage abundance and activation state following TNFα blockade.

While anti-TNFα antibody treatment had no significant effects on combined histolopathological score, decreases in the number and severity of fibrotic foci in trichrome stained sections were observed when compared to bleomycin only groups at 21 d. These findings are in contrast to previous reports demonstrating that TNFα inhibition reduces inflammation and/or fibrosis induced by a number of diverse pulmonary toxicants including bleomycin (Piguet et al., 1989; Piguet and Vesin, 1994; Shvedova et al., 1994; Lee et al., 2017; Ntusi et al., 2018). It is possible that the limited effects observed acutely in our studies are due to the intravenous route of administration of the anti-TNFα antibody. It may also be that additional doses of anti-TNFα antibody are required to block inflammation, a notion supported by our findings of reduced fibrosis at 21 d post bleomycin after four doses of the antibody. Such a repetitive therapeutic approach would be viable in humans as anti-TNFα antibodies are used chronically with biweekly injections in diseases such as rheumatoid arthritis.

Despite limited effects on overall histopathology, anti-TNFα antibody therapy successfully rescued Type II alveolar epithelial cell function. Type II epithelial cells produce both the surfactant portion of the lung lining fluid, namely the phospholipids, and the surface-active proteins and collectins, SP-A, -–B, -–C, and -–D. To assess these separate functions, we measured BAL levels of phospholipids and SP-B, along with SP-D during the fibrotic phase

of injury. We found a reduction in the phospholipid-to-SP-B ratio following bleomycin administration, indicating dysregulation of surface tension and increased work of breathing (Massa et al., 2017). These findings are consistent with previous findings of lung lining fluid changes following lung injury induced by bleomycin, where reductions in relative SP-B content were related to increased lung collapse and reduced lung function (Savani et al., 2001; Knudsen et al., 2018). Treatment with anti-TNFα antibody was found to increase phospholipid, SP-B, and SP-D levels, and to normalize the phospholipid-to-SP-B ratio. These data suggest an overall upregulation of type II cell function both in the production of surface-active material (phospholipids and SP-B), but also in the production of immunoregulatory collectin (SP-D). Improved type II cell function may be protective against lung injury, a notion supported by previous studies demonstrating a reduction in bleomycin-injury and fibrosis following administration of anti-TNFα antibody (Piguet et al., 1989; Piguet and Vesin, 1994)

Our flow cytometric BAL analysis highlighted two populations of $F4/80^+$ myeloid cells: one consisting of resident alveolar macrophages ($CD11c^+Cd11b^-$) and a second group including $CD11b^+$ infiltrating macrophages (Misharin et al., 2013; Zaynagetdinov et al., 2013). Alveolar macrophages are responsible for homeostatic maintenance and early response to exogenous stressors (Joshi et al., 2018). Bleomycin-induced increases in CD206, but not Ly6C, in alveolar macrophages is indicative of a more reparative function of these cells (Grabarz et al., 2018). We also found that CD206 levels in alveolar macrophages increased with time, supporting the idea that fibrotic remodeling is correlated with expression of this scavenger receptor (Wynn and Vannella, 2016). Anti-TNFα antibody treatment had no effect on the abundance of $CD206^+$ or $Ly6C^+$ resident alveolar macrophages.

Flow cytometric analysis of $CD11b^+$ infiltrating cells confirmed our immunohistochemical findings of prolonged accumulation of these cells in the lung following bleomycin administration. This response was greater in the anti-TNFα antibody treated group, indicating that the drug modulated the response of peripheral myeloid subsets. Recent evidence suggested that alveolar macrophages developing from monocytic precursors, termed monocyte-derived alveolar macrophages, are involved in tissue remodeling and fibrosis (Misharin et al., 2017; Joshi et al., 2020). Our findings that BAL $CD11b^+$ cells upregulate expression of CD11c and CD206 expression over time, support the notion that as these cells mature, they develop an anti-inflammtory/pro-fibrotic phenotype (Gonzalez-Juarrero et al., 2003; Misharin et al., 2014). This progression was unaltered by antibody treatment, suggesting that TNFα does not influence the transition to a mature ($CD11c^+$) and possibly pro-fibrotic (CD206) phenotype.

Interstitial macrophages represent another lung resident population distinct from alveolar macrophages in ontogeny, phenotype, and function (Tan and Krasnow, 2016; Gibbings et al., 2017; Liegeois et al., 2018; Schyns et al., 2019). This macrophage subset is replenished largely from circulating monocytes during homeostatic and stressful conditions. CD11b has been reported to be expressed by interstitial macrophages (Liegeois et al., 2018). To examine bleomycin-induced changes in interstitial macrophages, free from confounding blood monocytes and alveolar macrophages, we thoroughly perfused the lungs after bronchoalveolar lavage. This was followed by collagenase digestion and magnetic

selection of F4/80$^+$ cells. Our results demonstrated no significant changes in the abundance of CD11b$^+$ interstitial macrophages in the lung following bleomycin administration, or after anti-TNFα antibody treatment. In accord with recent published gating strategies (Gibbings et al., 2017), we identified two populations of interstitial macrophages defined by their differential expression of the maturation marker, CD11c. The subset lacking CD11c expression was designated as immature interstitial macrophages. Our data show reduced numbers of immature interstitial macrophages (CD11b$^+$CD11c$^-$) at 21 d post exposure, a shift likely indicating a transition to a mature phenotype at a time coordinate with fibrogenesis. Phenotypic analysis of CD11b$^+$CD11c$^+$ and CD11b$^+$CD11c$^-$ (immature) interstitial macrophages identified time related increases in CD206 expression following bleomycin exposure. Conversely, immature interstitial macrophages expressed significantly lower levels of the pro-inflammatory marker, Ly6C 21 days post bleomycin. Our observation that anti-TNFα treatment reduced the relative abundance of Ly6C$^+$ interstitial macrophages 7 days post bleomycin exposure, combined with blunted accumulation of CD206$^+$ immature interstitial macrophages at 21 days, supports the notion that anti-TNFα antibody therapy effectively limits both pro- inflammatory (Ly6C) and pro-fibrotic (CD206) activation in the lung interstitium (Greiffo et al., 2016; Misharin et al., 2017; Schyns et al., 2018).

In summary, the results of our studies demonstrate that bleomycin produces persistent lung injury, progressing to fibrosis. This is accompanied by epithelial cell dysfunction and macrophage activation both within the lung lining (BAL) and the interstitium (digest). Anti-TNFα antibody therapy produced significant improvement in type II cell function and affected interstitial macrophage influx and activation. Together, these results support the idea that therapies aimed at improving work of breathing and interstitial cell function may represent an effective strategy to treat inflammation-induced fibrosis.

Supplementary Material

Refer to Web version on PubMed Central for supplementary material.

Funding

This work is supported by HL086621 (AJG), ES007148 (TNG), GM108463 (TNG), ES019851 (TNG).

References

Aggarwal BB, 2003. Signalling pathways of the TNF superfamily: a double-edged sword. Nat. Rev. Immunol 3, 745–756. [PubMed: 12949498]

Barkauskas CE, Noble PW, 2014. Cellular mechanisms of tissue fibrosis. 7. New insights into the cellular mechanisms of pulmonary fibrosis. Am. J. Phys. Cell Phys 306, C987–C996.

Bhalla DK, Reinhart PG, Bai C, Gupta SK, 2002. Amelioration of ozone-induced lung injury by anti-tumor necrosis factor-alpha. Toxicol. Sci 69, 400–408. [PubMed: 12377989]

Blaser H, Dostert C, Mak TW, Brenner D, 2016. TNF and ROS crosstalk in inflammation. Trends Cell Biol. 26, 249–261. [PubMed: 26791157]

Bligh EG, Dyer WJ, 1959. A rapid method of total lipid extraction and purification. Can. J. Biochem. Physiol 37, 911–917. [PubMed: 13671378]

Braga TT, Correa-Costa M, Azevedo H, Silva RC, Cruz MC, Almeida MES, Hiyane MI, Moreira-Filho CA, Santos MF, Perez KR, Cuccovia IM, Camara NOS, 2016. Early infiltration of

p40IL12(+)CCR7(+)CD11b(+) cells is critical for fibrosis development. Immun. Inflamm. Dis 4, 300–314. [PubMed: 27621813]

Cao Y, Tao J-Q, Bates SR, Beers MF, Haczku A, 2004. IL-4 induces production of the lung collectin surfactant protein-D. J. Allergy Clin. Immunol 113, 439–444. [PubMed: 15007344]

Casey J, Kaplan J, Atochina-Vasserman EN, Gow AJ, Kadire H, Tomer Y, Fisher JH, Hawgood S, Savani RC, Beers MF, 2005. Alveolar surfactant protein D content modulates bleomycin-induced lung injury. Am. J. Respir. Crit. Care Med 172, 869–877. [PubMed: 15994463]

Ge V, Banakh I, Tiruvoipati R, Haji K, 2018. Bleomycin-induced pulmonary toxicity and treatment with infliximab: a case report. Clin. Case Rep 6, 2011–2014. [PubMed: 30349718]

Gibbings SL, Thomas SM, Atif SM, McCubbrey AL, Desch AN, Danhorn T, Leach SM, Bratton DL, Henson PM, Janssen WJ, Jakubzick CV, 2017. Three unique interstitial macrophages in the murine lung at steady state. Am. J. Respir. Cell Mol. Biol 57, 66–76. [PubMed: 28257233]

Gonzalez-Juarrero M, Shim TS, Kipnis A, Junqueira-Kipnis AP, Orme IM, 2003. Dynamics of macrophage cell populations during murine pulmonary tuberculosis. J. Immunol 171, 3128–3135. [PubMed: 12960339]

Grabarz F, Aguiar CF, Correa-Costa M, Braga TT, Hyane MI, Andrade- Oliveira V, Landgraf MA, Camara NOS, 2018. Protective role of NKT cells and macrophage M2-driven phenotype in bleomycin-induced pulmonary fibrosis. Inflammopharmacology 26, 491–504. [PubMed: 28779430]

Greiffo F, Fernandez I, Frankenberger M, Behr J, Eickelberg O, 2016. Circulating monocytes from interstitial lung disease patients show an activated phenotype. Eur. Respir. J 48, PA3894.

Guo C, Atochina-Vasserman E, Abramova H, George B, Manoj V, Scott P, Gow A, 2016. Role of NOS2 in pulmonary injury and repair in response to bleomycin. Free Radic Biol Med 91, 293–301. 10.1016/j.freeradbiomed.2015.10.417. [PubMed: 26526764]

Guttentag SH, Bieler BM, Beers MF, Ballard PL, 1997. Surfactant ProteinB (SPB) processing is regulated by glucocorticoids in human fetal type 2 cells. Pediatr. Res 41, 46.

Hay J, Shahzeidi S, Laurent G, 1991. Mechanisms of bleomycin-induced lung damage. Arch. Toxicol 65, 81–94. [PubMed: 1711838]

Izbicki G, Segel MJ, Christensen TG, Conner MW, Breuer R, 2002. Time course of bleomycin-induced lung fibrosis. Int. J. Exp. Pathol 83, 111–119.

Joshi N, Walter JM, Misharin AV, 2018. Alveolar macrophages. Cell. Immunol 330, 86–90. [PubMed: 29370889]

Joshi N, Watanabe S, Verma R, Jablonski RP, Chen C-I, Cheresh P, Markov NS, Reyfman PA, McQuattie-Pimentel AC, Sichizya L, Lu Z, Piseaux-Aillon R, Kirchenbuechler D, Flozak AS, Gottardi CJ, Cuda CM, Perlman H, Jain M, Kamp DW, Budinger GRS, Misharin AV, 2020. A spatially restricted fibrotic niche in pulmonary fibrosis is sustained by M-CSF/M-CSFR signalling in monocyte- derived alveolar macrophages. Eur. Respir. J 55, 1900646.

Knudsen L, Lopez-Rodriguez E, Berndt L, Steffen L, Ruppert C, Bates JHT, Ochs M, Smith BJ, 2018. Alveolar micromechanics in bleomycin-induced lung injury. Am. J. Respir. Cell Mol. Biol 59, 757–769. [PubMed: 30095988]

Kobayashi Y, 2010. The regulatory role of nitric oxide in proinflammatory cytokine expression during the induction and resolution of inflammation. J. Leukoc. Biol 88, 1157–1162. [PubMed: 20807706]

Koyama K, Goto H, Morizumi S, Kagawa K, Nishimura H, Sato S, Kawano H, Toyoda Y, Ogawa H, Homma S, Nishioka Y, 2019. The tyrosine kinase inhibitor TAS-115 attenuates bleomycin-induced lung fibrosis in mice. Am. J. Respir. Cell Mol. Biol 60, 478–487. [PubMed: 30540913]

Laskin DL, Malaviya R, Laskin JD, 2019. Role of macrophages in acute lung injury and chronic fibrosis induced by pulmonary toxicants. Toxicol. Sci 168, 287–301. [PubMed: 30590802]

Lee J, Lee S, Zhang H, Hill MA, Zhang C, Park Y, 2017. Interaction of IL-6 and TNF-α contributes to endothelial dysfunction in type 2 diabetic mouse hearts. PLoS One 12, e0187189.

Liegeois M, Legrand C, Desmet CJ, Marichal T, Bureau F, 2018. The interstitial macrophage: a long-neglected piece in the puzzle of lung immunity. Cell. Immunol 330, 91–96. [PubMed: 29458975]

Malaviya R, Sunil VR, Venosa A, Verissimo VL, Cervelli JA, Vayas KN, Hall L, Laskin JD, Laskin DL, 2015. Attenuation of nitrogen mustard-induced pulmonary injury and fibrosis by anti-tumor necrosis factor-α antibody. Toxicol. Sci 148, 71–88. [PubMed: 26243812]

Malaviya R, Laskin JD, Laskin DL, 2017. Anti-TNFα therapy in inflammatory lung diseases. Pharmacol. Ther 180, 90–98. [PubMed: 28642115]

Massa CB, Groves AM, Jaggernauth SU, Laskin DL, Gow AJ, 2017. Histologic and biochemical alterations predict pulmonary mechanical dysfunction in aging mice with chronic lung inflammation. PLoS Comput. Biol 13, e1005570.

Misharin AV, Morales-Nebreda L, Mutlu GM, Budinger GR, Perlman H, 2013. Flow cytometric analysis of macrophages and dendritic cell subsets in the mouse lung. Am. J. Respir. Cell Mol. Biol 49, 503–510. [PubMed: 23672262]

Misharin AV, Cuda CM, Saber R, Turner JD, Gierut AK, Haines GK 3rd, Berdnikovs S, Filer A, Clark AR, Buckley CD, Mutlu GM, Budinger GR, Perlman H, 2014. Nonclassical Ly6C(−) monocytes drive the development of inflammatory arthritis in mice. Cell Rep. 9, 591–604. [PubMed: 25373902]

Misharin AV, Morales-Nebreda L, Reyfman PA, Cuda CM, Walter JM, McQuattie-Pimentel AC, Chen CI, Anekalla KR, Joshi N, Williams KJN, Abdala-Valencia H, Yacoub TJ, Chi M, Chiu S, Gonzalez-Gonzalez FJ, Gates K, Lam AP, Nicholson TT, Homan PJ, Soberanes S, Dominguez S, Morgan VK, Saber R, Shaffer A, Hinchcliff M, Marshall SA, Bharat A, Berdnikovs S, Bhorade SM, Bartom ET, Morimoto RI, Balch WE, Sznajder JI, Chandel NS, Mutlu GM, Jain M, Gottardi CJ, Singer BD, Ridge KM, Bagheri N, Shilatifard A, Budinger GRS, Perlman H, 2017. Monocyte-derived alveolar macrophages drive lung fibrosis and persist in the lung over the life span. J. Exp. Med 214, 2387–2404. [PubMed: 28694385]

Moeller A, Ask K, Warburton D, Gauldie J, Kolb M, 2008. The bleomycin animal model: a useful tool to investigate treatment options for idiopathic pulmonary fibrosis? Int. J. Biochem. Cell Biol 40, 362–382. [PubMed: 17936056]

Mosser DM, Edwards JP, 2008. Exploring the full spectrum of macrophage activation. Nat. Rev. Immunol 8, 958–969. [PubMed: 19029990]

Mukhopadhyay S, Hoidal JR, Mukherjee TK, 2006. Role of TNFalpha in pulmonary pathophysiology. Respir. Res 7, 125. [PubMed: 17034639]

Ntusi NAB, Francis JM, Sever E, Liu A, Piechnik SK, Ferreira VM, Matthews PM, Robson MD, Wordsworth PB, Neubauer S, Karamitsos TD, 2018. Anti-TNF modulation reduces myocardial inflammation and improves cardiovascular function in systemic rheumatic diseases. Int. J. Cardiol 270, 253–259. [PubMed: 30017519]

Piguet PF, Vesin C, 1994. Treatment by human recombinant soluble TNF receptor of pulmonary fibrosis induced by bleomycin or silica in mice. Eur. Respir. J 7, 515–518. [PubMed: 7516893]

Piguet PF, Collart MA, Grau GE, Kapanci Y, Vassalli P, 1989. Tumor necrosis factor/cachectin plays a key role in bleomycin-induced pneumopathy and fibrosis. J. Exp. Med 170, 655–663. [PubMed: 2475571]

Roszer T, 2015. Understanding the mysterious M2 macrophage through activation markers and effector mechanisms. Mediat. Inflamm 2015, 816460.

Rouser G, Siakotos AN, Fleischer S, 1966. Quantitative analysis of phospholipids by thin-layer chromatography and phosphorus analysis of spots. Lipids 1, 85–86. [PubMed: 17805690]

Saito K, Tanaka N, Ikari J, Suzuki M, Anazawa R, Abe M, Saito Y, Tatsumi K, 2019. Comprehensive lipid profiling of bleomycin-induced lung injury. J. Appl. Toxicol 39, 658–671. [PubMed: 30565269]

Savani RC, Godinez RI, Godinez MH, Wentz E, Zaman A, Cui Z, Pooler PM, Guttentag SH, Beers MF, Gonzales LW, Ballard PL, 2001. Respiratory distress after intratracheal bleomycin: selective deficiency of surfactant proteins B and C. Am. J. Phys. Lung Cell. Mol. Phys 281, L685–L696.

Schyns J, Bureau F, Marichal T, 2018. Lung interstitial macrophages: past, present, and future. J Immunol Res 2018, 5160794.

Schyns J, Bai Q, Ruscitti C, Radermecker C, De Schepper S, Chakarov S, Farnir F, Pirottin D, Ginhoux F, Boeckxstaens G, Bureau F, Marichal T, 2019. Non- classical tissue monocytes and

two functionally distinct populations of interstitial macrophages populate the mouse lung. Nat. Commun 10, 3964. [PubMed: 31481690]

Shariati S, Kalantar H, Pashmforoosh M, Mansouri E, Khodayar MJ, 2019. Epicatechin protective effects on bleomycin-induced pulmonary oxidative stress and fibrosis in mice. Biomed. Pharmacother 114, 108776.

Shvedova AA, Kramarik JA, Keohavong P, Chumakov KM, Karol MH, 1994. Use of anti-TNF-alpha antiserum to investigate toxic alveolitis arising from cotton dust exposure. Exp. Lung Res 20, 297–315. [PubMed: 7988494]

Soldano S, Pizzorni C, Paolino S, Trombetta AC, Montagna P, Brizzolara R, Ruaro B, Sulli A, Cutolo M, 2016. Alternatively activated (M2) macrophage phenotype is inducible by endothelin-1 in cultured human macrophages. PLoS One 11, e0166433.

Tan SY, Krasnow MA, 2016. Developmental origin of lung macrophage diversity. Development 143, 1318–1327. [PubMed: 26952982]

Venosa A, Malaviya R, Choi H, Gow AJ, Laskin JD, Laskin DL, 2016. Characterization of distinct macrophage subpopulations during nitrogen mustard- induced lung injury and fibrosis. Am. J. Respir. Cell Mol. Biol 54, 436–446. [PubMed: 26273949]

Walters DM, Kleeberger SR, 2008. Mouse models of bleomycin-induced pulmonary fibrosis. Curr. Protoc. Pharmacol 40 (1), 5.46.1–5.46.17. Chapter 5, Unit 5.46.

Williamson JD, Sadofsky LR, Hart SP, 2015. The pathogenesis of bleomycin- induced lung injury in animals and its applicability to human idiopathic pulmonary fibrosis. Exp. Lung Res 41, 57–73. [PubMed: 25514507]

Wynn TA, Vannella KM, 2016. Macrophages in tissue repair, regeneration, and fibrosis. Immunity 44, 450–462. [PubMed: 26982353]

Yang Z, Ming X-F, 2014. Functions of arginase isoforms in macrophage inflammatory responses: impact on cardiovascular diseases and metabolic disorders. Front. Immunol 5, 533. [PubMed: 25386179]

Yu Z, Yan B, Gao L, Dong C, Zhong J, Nguyen B, Seong Lee S, Hu X, Liang F, 2016. Targeted delivery of bleomycin: a comprehensive anticancer review. Curr. Cancer Drug Targets 16, 509–521. [PubMed: 26632436]

Zaynagetdinov R, Sherrill TP, Kendall PL, Segal BH, Weller KP, Tighe RM, Blackwell TS, 2013. Identification of myeloid cell subsets in murine lungs using flow cytometry. Am. J. Respir. Cell Mol. Biol 49, 180–189. [PubMed: 23492192]

Zhang LM, Zhang Y, Fei C, Zhang J, Wang L, Yi ZW, Gao G, 2019. Neutralization of IL-18 by IL-18 binding protein ameliorates bleomycin-induced pulmonary fibrosis via inhibition of epithelial-mesenchymal transition. Biochem. Biophys. Res. Commun 508, 660–666. [PubMed: 30527805]

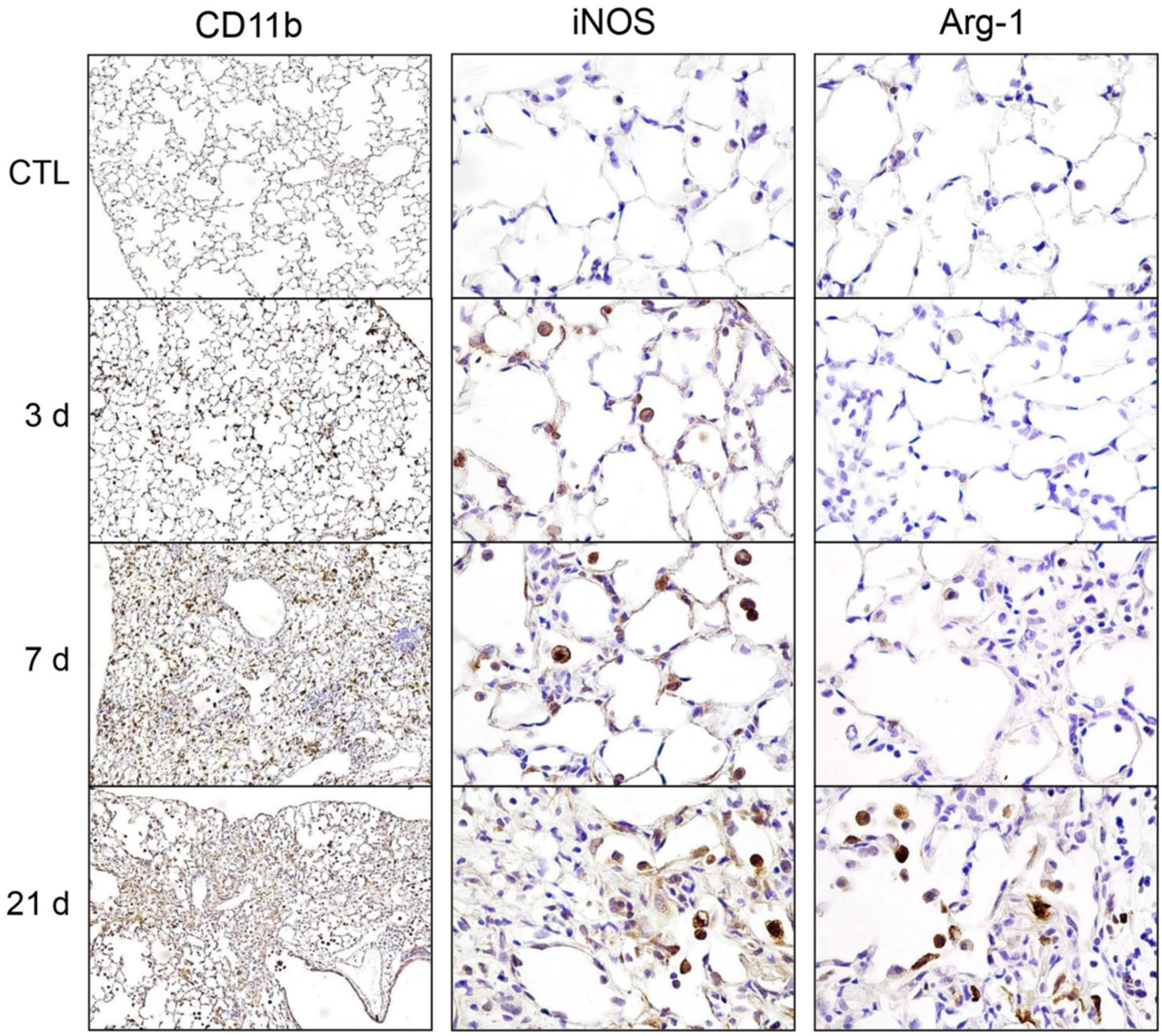

Fig. 1.

Effects of bleomycin on lung inflammation and macrophage activation. Lung sections, prepared 0 d (CTL), 3 d, 7 d, and 28 d after exposure of mice to bleomycin (3 U/kg), were immunostained with antibody to CD11b (left panels, 100× magnification), iNOS (center panels, 400× magnification), and Arg-1 (right panels, 400× magnification). Binding was visualized using a Vectastain kit. Representative sections from 3 mice/treatment group are shown.

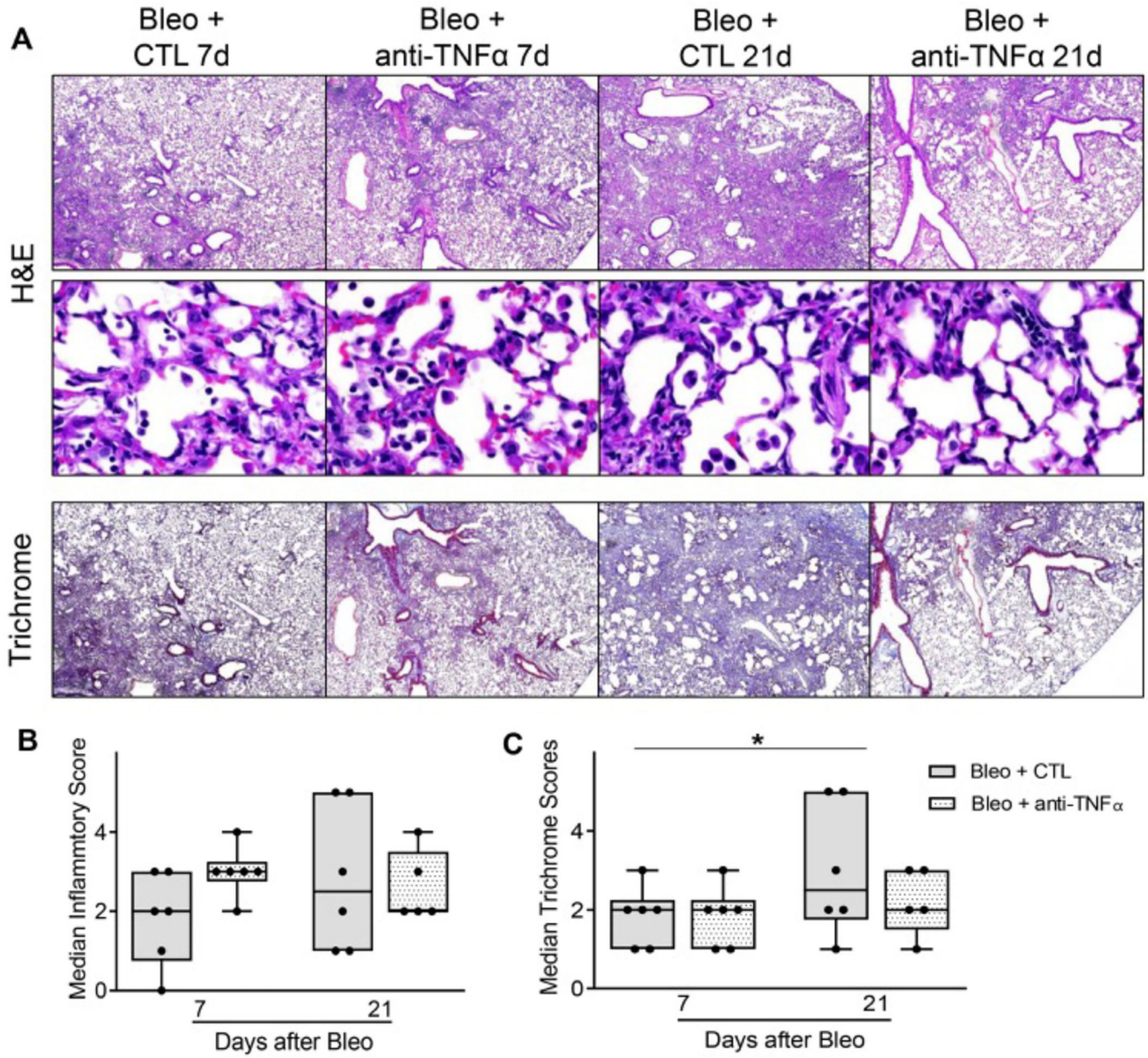

Fig. 2.

Effects of anti-TNFα antibody on bleomycin-induced lung histolopathology and cell counts. *Panel A:* Hematoxylin and Eosin and Masson's Trichrome stain of tissue sections were prepared 7 d, and 21 d after exposure of mice to bleomycin (Bleo + CTL) or Bleo + anti-TNFα antibody. Original magnification: 40× (top and bottom panels) and 400× (middle panels). Representative images from at least 3 mice/treatment group are shown. *Panels B and C:* Histopathological scoring of sections was based on qualitative score of perivascular and peribronchial infiltrate, edema, number and extent of injury foci, alveolar thickening. Data are represented as median scores. *Significantly different ($p \leq 0.05$) from Bleo + CTL group.

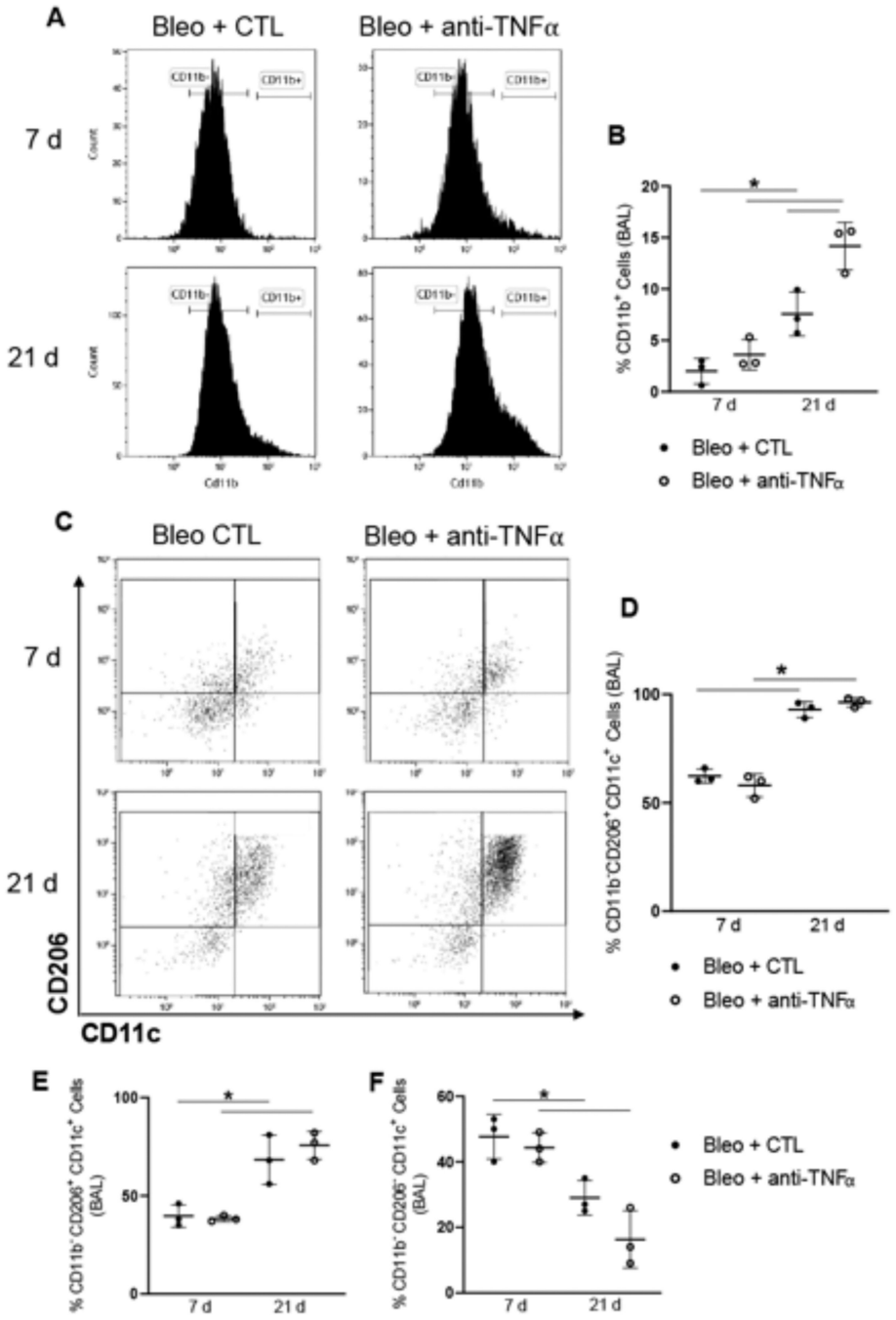

Fig. 3.

Effects of anti-TNFα antibody on bleomycin-induced macrophage accumulation and activation in BAL. *Panel A:* Representative histogram of CD11b expression by F4/80$^+$ BAL cells following Bleo + CTL or Bleo + anti-TNFα administration. *Panel B:* Quantification of CD11b$^+$ cells collected 7 d and 21 d following Bleo + CTL or Bleo + anti-TNFα antibody administration. Data are mean ± SD (n = 3). *Panels C-F:* Expression of CD206 and CD11c by CD11b$^+$ cells (*Panels C and D*) and by CD11b$^-$ cells (*Panels E and F*) 7 d and 21 d post

Bleo + CTL or Bleo + anti-TNFα. Bars, mean ± SD (n = 3). *Significantly different ($p \leq 0.05$) from other groups

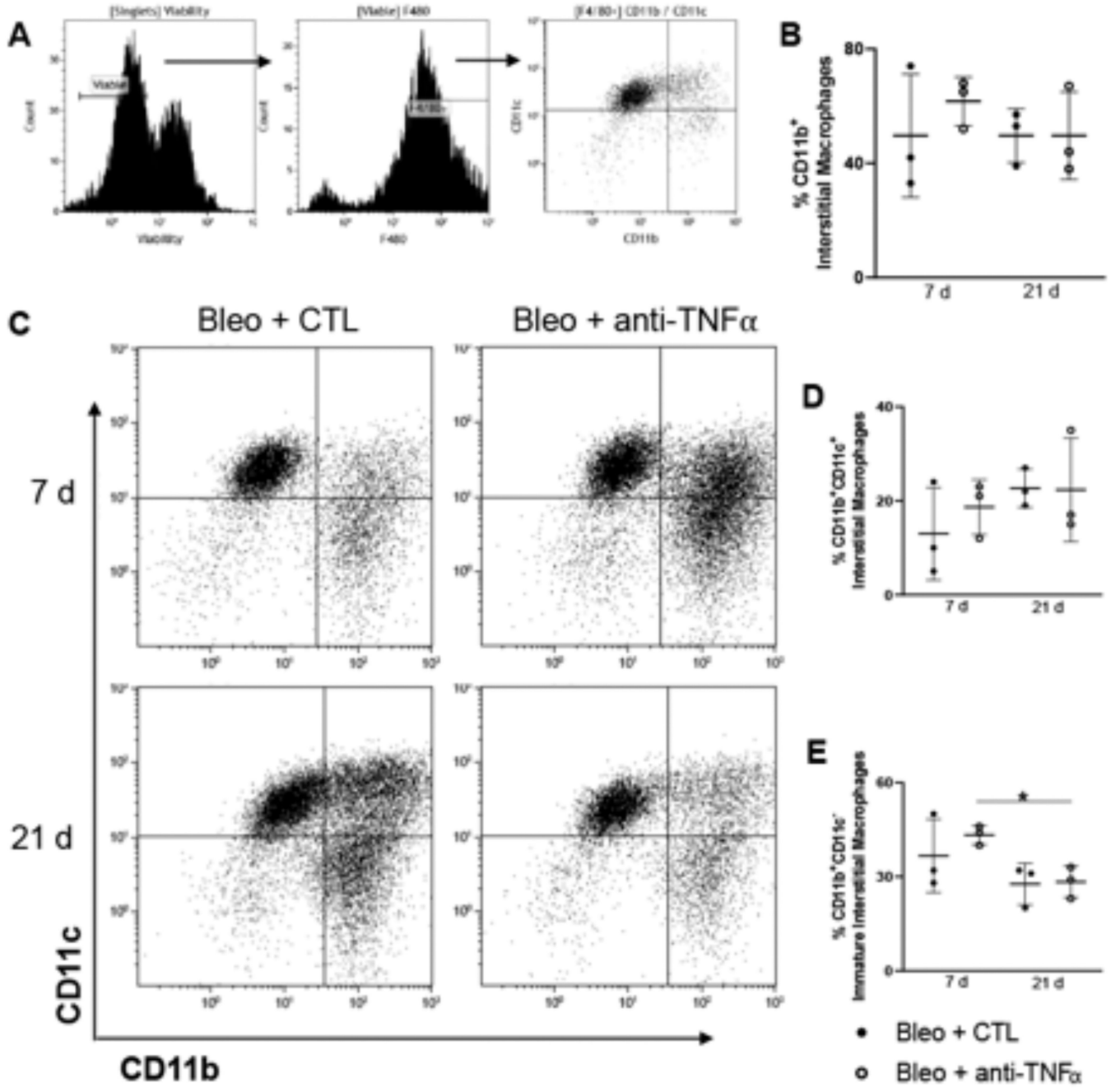

Fig. 4.

Effects of anti-TNFα antibody administration on bleomycin-induced macrophage mobilization and activation in lung tissue. *Panel A:* Gating strategy used to identify myeloid subsets following F4/80 magnetic selection of collagenase digested tissue collected 7 d and 21 d post Bleo + CTL or Bleo + anti-TNFα exposure. *Panel B:* Quantification of total CD11b Interstitial Macrophages *Panel C-E:* Representative dot plot for CD11b and CD11c cells 7 d and 21 d post Bleo + CTL or Bleo + anti-TNFα exposure (*Panel C*); $CD11b^{+}CD11c^{+}$, interstitial macrophages (*Panel D*); and $CD11b^{+}CD11c^{-}$, immature macrophages (*panel E*) in the tissue 7 d and 21 d post Bleo + CTL or Bleo + anti-TNFα

exposure. Data are represented as mean ± SD (n = 3). *Significantly different ($p \leq 0.05$) from other groups.

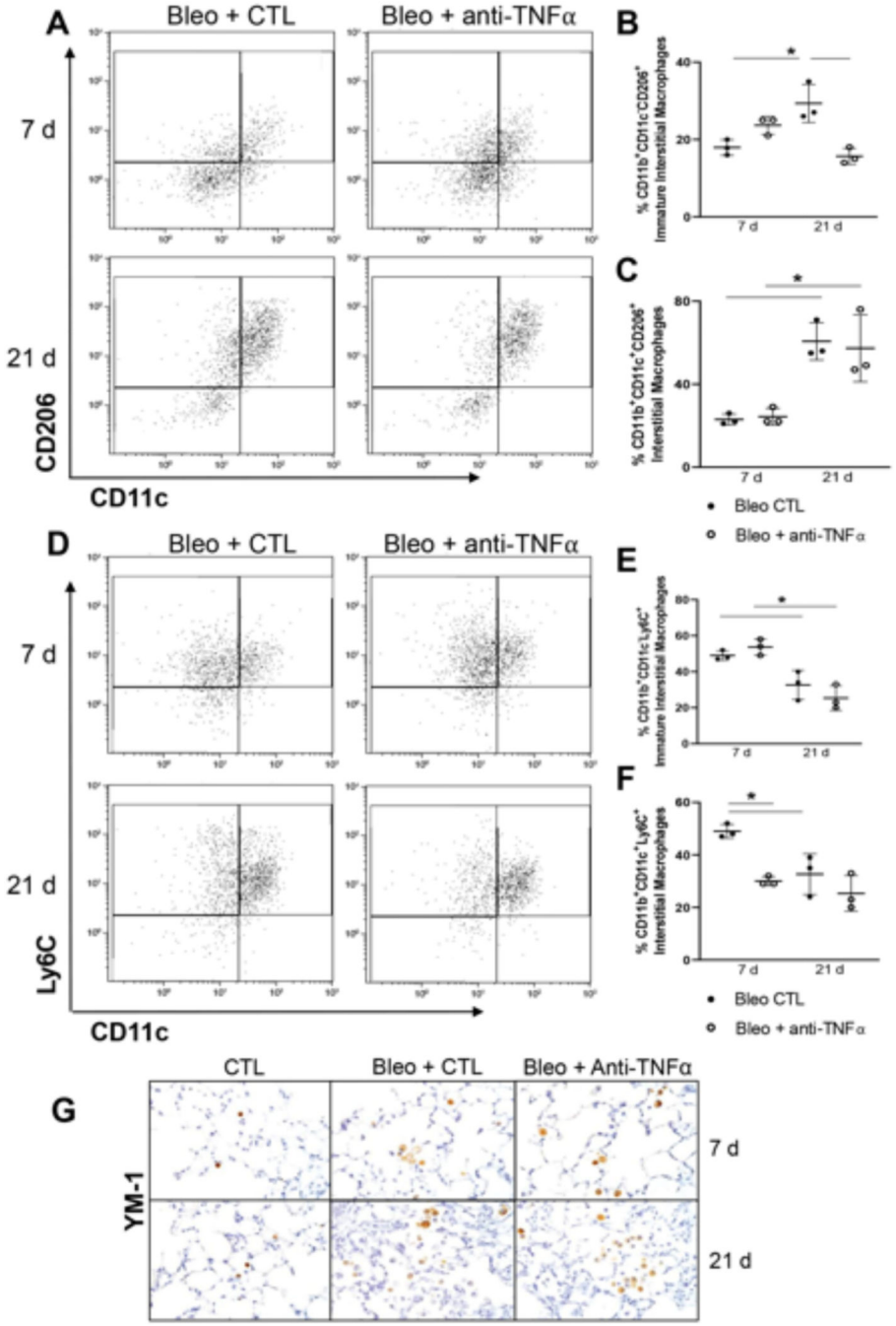

Fig. 5.

Effects of anti-TNFα administration on bleomycin-induced macrophage phenotype in lung tissue. *Panel A:* Representative dot plot for CD206 and CD11c cells 7 d and 21 d post Bleo CTL or Bleo + anti-TNFα exposure. *Panel B-C:* Quantification of $CD206^{+}$ in $CD11b^{+}CD11c^{-}$, immature interstitial macrophages (*Panel B*), and $CD11b^{+}CD11c^{+}$, interstitial macrophages (*Panel C*), in the tissue 7 d and 21 d post Bleo + CTL or Bleo + anti-TNFα exposure. Data are represented as mean ± SD (n = 3). *Panel D:* Representative dot plot for Ly6C and CD11c cells 7 d and 21 d post Bleo + CTL or Bleo + anti-TNFα

exposure. *Panel E-F:* Quantification of immature $Ly6C^{+}CD11c^{-}$ (*Panel E*), and mature $Ly6C^{+}CD11c^{+}$ (*Panel F*) interstitial macrophages in the tissue 7 d and 21 d post Bleo + CTL or Bleo + anti-TNFα exposure. Data are mean ± SD (n = 3). *Panel G:* Lung sections, prepared 7 d and 21 d after exposure to Bleo + CTL or Bleo + anti-TNFα, were immunostained with antibody to YM-1. Binding was visualized using a Vectastain kit. Original magnification, 400×. Representative sections from 3 mice/treatment group are shown. *Significantly different ($p \leq 0.05$) from other groups.

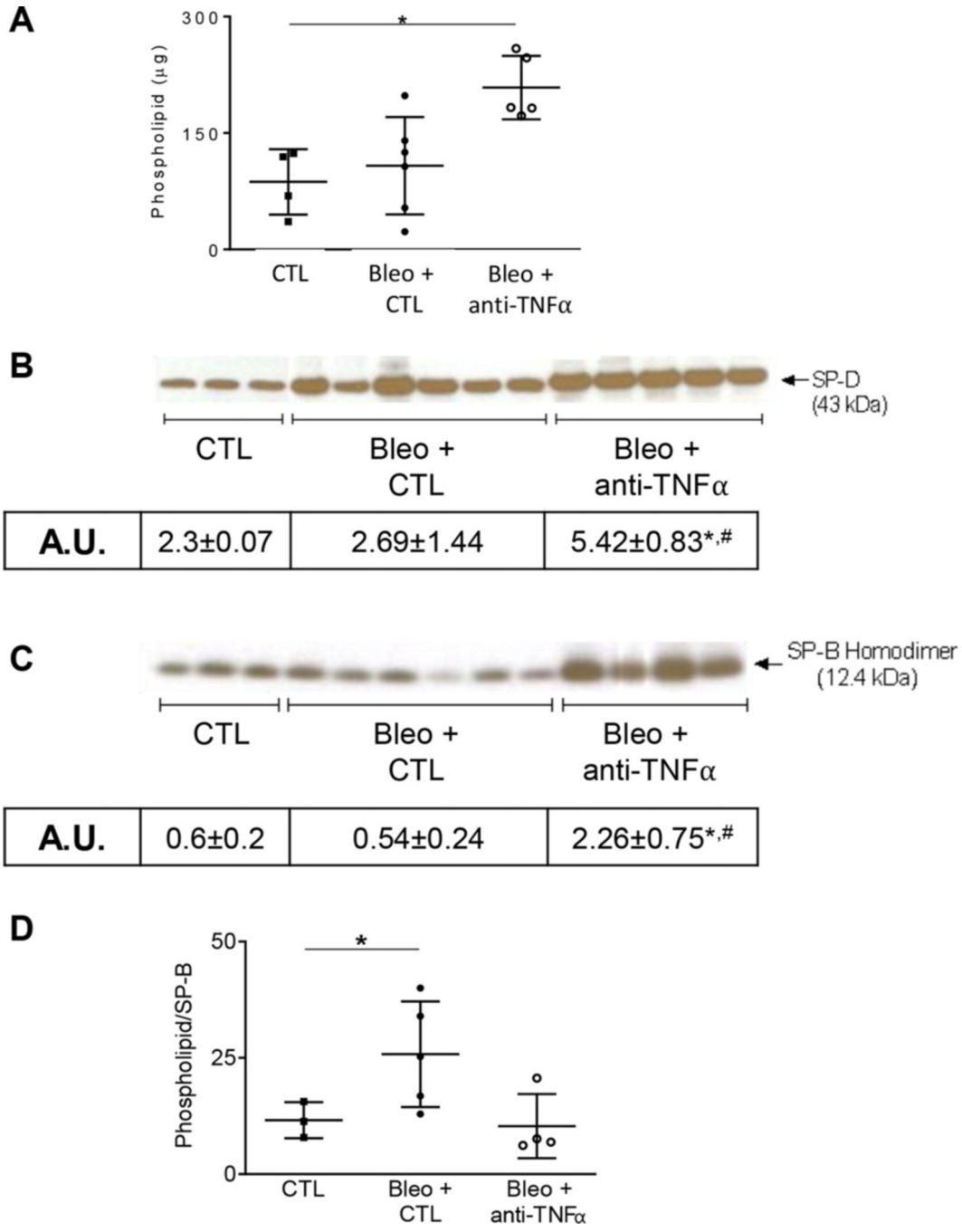

Fig. 6.

Effects of anti-TNFα administration on bleomycin-induced alterations in surfactant protein expression. *Panels A-C:* Whole BAL and large aggregate fractions, collected at 0 d (CTL) and 21 d after exposure to Bleo + CTL or Bleo + anti-TNFα, were assessed for total phospholipid content (*Panel A*), SP-D (*Panel B*) and SP-B (*Panel C*) by western blot analysis, respectively. *Panel D:* Total Phospholipid-to-SP-B ratio at 0 d (CTL) and 21 d after exposure to Bleo + CTL or Bleo + anti-TNFα, representing a biomarker for type II cell function. Quantification of expression was performed using ImageJ and represented as

arbitrary unit (A.U.) and represented as mean ± SD (n = 3–6). *Significantly different ($p \leq 0.05$) from other groups.